

Variational mechanics of water at biological interfaces

Ariel Fernández

Instituto Argentino de Matemática, CONICET, Buenos Aires, C1083ACA, Argentina

Department of Computer Science, The University of Chicago,

Chicago, IL 60637, USA

Phone: 713 299 1233; E-mail: ariel@uchicago.edu

A variational principle governing nanoscale water configurations at biological interfaces is derived. The underlying functional determines a scalar field $g=g(\mathbf{r})$ indicating the expected hydrogen-bond coordination of water at position \mathbf{r} , and includes an elastic term to penalize local coordination losses. The minimization of interfacial free energy implies that g must obey a Poisson-type equation with Dirichlet boundary conditions. The equation is integrated and the specialization of the treatment to protein-water interfaces enables the determination of protein complexation propensities and the identification of protein binding sites and binding hot spots.

PACS numbers: 87.15.Aa, 61.20.Qg, 41.20.Cv

Running Title: Variational water mechanics

1. Introduction

In spite of significant progress [1-4], the physical underpinnings of biological-water interfaces remain elusive, hindering our understanding of biomolecular associations [5-9]. The partial confinement of interfacial water within inhomogeneous nanoscale cavities makes it difficult to define thermodynamic concepts like interfacial tension, useful to describe homogeneous phase separation [10, 11]. In aqueous biological contexts, the interfacial physics is complex, as solutes associate forming complexes but do not precipitate. The only known phase separations for natural soluble proteins under physiological conditions are neurodegenerative fibrillogenic aggregates, involving misfolded prions [9].

This work addresses the problem of computing interfacial tension in biomolecular contexts and validates the results by identifying protein binding sites without resorting to information on homologous proteins or knowledge-based potentials [12]. Strikingly, the treatment singles out the soluble prion protein structure as possessing the highest protein-water interfacial tension. Befitting a nanoscale description, the theoretical derivation introduces an elastic term that penalizes local changes in hydrogen-bonding coordination and allows for compensations to this elastic penalization as water dipoles interact with pre-existing or induced electrostatic fields yielding a more or less restricted polarization depending on their local coordination environments.

2. Variational mechanics of water at the biological interface

To compute interfacial tension, we adopt the field $g=g(\mathbf{r})$, a descriptor that assigns to each position vector \mathbf{r} the expected value of hydrogen-bond coordination of a water molecule situated within a sphere centered at position \mathbf{r} with radius 2.5\AA (thickness of a single water layer [13, 14]). This radius spans a van der Waals radius plus half a hydrogen-bond distance. The $g(\mathbf{r})$ value is computed as time average over solvent configurations determined by molecular dynamics over a 100ns-period after the protein structure is equilibrated with the solvent, thus allowing for breathing motions of exposed atoms [13].

Within this representation, the minimization of interfacial tension requires a variational principle, whereby the extremal of the surface integral $\Delta G_{\text{if}} = \int \Xi(\mathbf{g}(\mathbf{r}), \nabla \mathbf{g}(\mathbf{r})) d\mathbf{r}$ represents the free energy cost of spanning the protein-water (P-W) interface. Thus, $\Xi(\mathbf{g}(\mathbf{r}), \nabla \mathbf{g}(\mathbf{r})) d\mathbf{r}$ gives the free-energy cost of transferring water from bulk to volume $d\mathbf{r}$ at position \mathbf{r} . A hydrogen bond is defined by the geometric constraints: O-O distance $< 3.2\text{\AA}$ and O-H-O angle a_{HB} satisfying $120^\circ \leq a_{\text{HB}} \leq 180^\circ$. Compared with bulk water, interfacial water has reduced hydrogen-bonding opportunities ($g < g_{\text{bulk}} = 4$) and may counterbalance such losses by interacting with polar groups on the protein surface. Thus, the term ΔG_{if} incorporates unfavorable local decreases in g and favorable polarization contributions.

Exploiting the analogy with Lagrangian mechanics [10], we write $\Delta G_{\text{if}} = \int \frac{1}{2} \{ \lambda |\nabla \mathbf{g}|^2 - \mathbf{P}(\mathbf{g}(\mathbf{r}))^2 \} d\mathbf{r}$, where the elastic term $\frac{1}{2} \lambda |\nabla \mathbf{g}|^2$ accounts for tension-generating reductions in water coordination, and the polarization $\mathbf{P}(\mathbf{g}(\mathbf{r}))$ accounts for dipole-electrostatic field interactions. Bulk water properties are incorporated since the scaling parameter λ is obtained from the interfacial tension of a large nonpolar sphere with radius θ in the macroscopic limit $\theta/1\text{nm} \rightarrow \infty$. We get $\lambda = 9.0\text{mJ/m} = \lim_{\theta/1\text{nm} \rightarrow \infty} \gamma(4\pi\theta^2) / \int \frac{1}{2} |\nabla \mathbf{g}|^2 d\mathbf{r}$, where $\gamma = 72\text{mJ/m}^2$ is the macroscopic surface tension of water at 298K, and $\int |\nabla \mathbf{g}|^2 d\mathbf{r} = \frac{1}{2} 4^2 \text{m}^{-1} (4\pi\theta^2)$, since $\nabla \mathbf{g} \neq 0$ only close to the interface and the associated g -jump is 4 units in magnitude. Thus, unfavorable P-W hydrophobic interactions are accounted for through the positive elastic contribution $\int \frac{1}{2} \lambda |\nabla \mathbf{g}|^2 d\mathbf{r}$ which extrapolates to macroscopic dimensions.

To determine the g -dependence of polarization $\mathbf{P}=\mathbf{P}(\mathbf{r})$, we adopt the Fourier-conjugate wavenumber space (ω -space) and represent the dipole correlation kernel $K_p(\omega)$ and the electrostatic field $\mathbf{E}=\mathbf{E}(\mathbf{r})$ in this space. This representation is required to capture the entire dielectric loss spectrum occurring mostly within the microwave range ($10^{-3}\text{m} \leq \omega^{-1} \leq 0.3\text{m}$) [15, 16]. The biophysical experimental data analyzed required examining results at bulk wavelengths spanning several orders of magnitude and are best reproduced at bulk wavelength $\omega^{-1} \approx 0.03\text{m}$

(Fig. 1, inset). At fixed wavelength, \mathbf{P} and \mathbf{E} are proportional [17, 18], but the proportionality constant is generally ω -dependent [18], which introduces a significant departure from the Poisson-Boltzmann electrostatics (see below). In ω -space we get

$$F(\mathbf{P})(\omega) = K_p(\omega)F(\mathbf{E})(\omega) \quad (1)$$

where F denotes 3D-Fourier transform $F(\mathbf{f})(\omega) = (2\pi)^{-3/2} \int e^{i\omega \cdot \mathbf{r}} \mathbf{f}(\mathbf{r}) d\mathbf{r}$, and the kernel $K_p(\omega)$ is the Lorentzian $K_p(\omega) = (\epsilon_b - \epsilon_o) / [1 + (\tau(\mathbf{r})c)^2 |\omega|^2]$, with $\tau(\mathbf{r})c$ =local dielectric relaxation length, c =light speed, ϵ_b =bulk permittivity constant, ϵ_o =vacuum permittivity. For bulk water, we get $\tau = \tau_b \approx 100$ ps, and relaxation length $\tau_b c = \omega_b^{-1} \approx 0.03$ m, the microwave wavelength yielding the best fit with experimental data (Fig. 1-inset containing sensitivity analysis). Through the Lorentzian, the frequency dependence of bulk permittivity is subsumed into the normal distribution factor $[1 + (\tau(\mathbf{r})c)^2 |\omega|^2]^{-1}$ with $\tau(\mathbf{r}) \equiv \tau_b$. Since $\mathbf{P}(\mathbf{r})$ satisfies $\nabla \cdot (\epsilon_o \mathbf{E} + \mathbf{P})(\mathbf{r}) = \rho(\mathbf{r})$ ($\rho(\mathbf{r})$ =charge density distribution) [17], Eq. (1) yields the following equation in \mathbf{r} -space:

$$\nabla \cdot [\int F^{-1}(K)(\mathbf{r}-\mathbf{r}') \mathbf{E}(\mathbf{r}') d\mathbf{r}'] = \rho(\mathbf{r}), \quad (2)$$

with $K(\omega) = \epsilon_o + K_p(\omega)$. The convolution $\int F^{-1}(K)(\mathbf{r}-\mathbf{r}') \mathbf{E}(\mathbf{r}') d\mathbf{r}'$ captures the correlation of the dipoles with the electrostatic field. Eq. (2) is not the Poisson-Boltzmann equation, which requires *ad-hoc* proportionality between \mathbf{E} and \mathbf{P} .

Upon water confinement, the dielectric relaxation undergoes a frequency redshift arising from the reduction in hydrogen-bond partnerships that translates in a reduction in dipole orientation possibilities ($g(\mathbf{r}) < 4$, $\tau(\mathbf{r}) > \tau_b$) [18]. Thus, at position \mathbf{r} , the relaxation time is $\tau = \tau_b \exp(B(g(\mathbf{r}))/k_B T)$, where the kinetic barrier $B(g(\mathbf{r})) = -k_B T \ln(g(\mathbf{r})/4)$ yields $\tau(\mathbf{r}) = \tau_b (g(\mathbf{r})/4)^{-1}$.

To obtain the g -dependent polarization term $\mathbf{P}(\mathbf{r})$, we introduce the electrostatic potential $\Psi = -\Phi(\mathbf{r})$, with $\mathbf{E} = \nabla \Phi$. Thus, Eq. (2) reads in ω -space:

$$F(\Phi)(\omega) = F(\rho)(\omega) / [|\omega|^2 K(\omega)], \quad (3)$$

where $|\omega|^2$ is the Fourier conjugate of ∇^2 . Thus, \mathbf{E} is obtained from the inverse Fourier transform of Eq. (3):

$$\mathbf{E}(\mathbf{r}) = \nabla F^{-1}\{F(\rho)(\boldsymbol{\omega})/[|\boldsymbol{\omega}|^2 K(\boldsymbol{\omega})]\}(\mathbf{r}) = (2\pi)^{-3/2} \nabla \int d\boldsymbol{\omega} e^{-i\boldsymbol{\omega} \cdot \mathbf{r}} F(\rho)(\boldsymbol{\omega})/[|\boldsymbol{\omega}|^2 K(\boldsymbol{\omega})] \quad (4)$$

The negative potential $\Phi(\mathbf{r})$ is determined for a generic charge distribution:

$$\rho(\mathbf{r}) = \sum_{m \in L} 4\pi q_m \delta(\mathbf{r} - \mathbf{r}_m), \quad (5)$$

with L =set of charges on the protein surface labeled by index m , which in $\boldsymbol{\omega}$ -space reads:

$$F(\rho)(\boldsymbol{\omega}) = (2\pi)^{-3/2} \sum_{m \in L} 4\pi q_m \exp(i\boldsymbol{\omega} \cdot \mathbf{r}_m), \quad (6)$$

Thus, we obtain:

$$\Phi(\mathbf{r}) = (2\pi)^{-3/2} \sum_{m \in L} \int d\boldsymbol{\omega} e^{-i\boldsymbol{\omega} \cdot (\mathbf{r} - \mathbf{r}_m)} 4\pi q_m / [|\boldsymbol{\omega}|^2 K(\boldsymbol{\omega})], \quad (7)$$

Now the g -dependent polarization term $\mathbf{P}(\mathbf{r})$ is obtained from Eq. (7) and the definition $\mathbf{E} = \nabla \Phi$:

$$\begin{aligned} \mathbf{P}(\mathbf{r}) &= \int F^{-1}(K_p)(\mathbf{r} - \mathbf{r}') \mathbf{E}(\mathbf{r}') d\mathbf{r}' = \\ &= (2\pi)^{-3} \sum_{m \in L} \int d\mathbf{r}' F^{-1}(K_p)(\mathbf{r} - \mathbf{r}') \nabla_{\mathbf{r}'} \int d\boldsymbol{\omega} e^{-i\boldsymbol{\omega} \cdot (\mathbf{r}' - \mathbf{r}_m)} 4\pi q_m / [|\boldsymbol{\omega}|^2 K(\boldsymbol{\omega})], \end{aligned} \quad (8)$$

The field $(g, \nabla g)$ is extremal of $\Delta G_{if} = \int \Xi(g(\mathbf{r}), \nabla g(\mathbf{r})) d\mathbf{r} = \int \frac{1}{2} \{ \lambda |\nabla g|^2 - |\mathbf{P}(g(\mathbf{r}))|^2 \} d\mathbf{r}$ if the spatial version of the Euler-Lagrange equation [10] holds:

$$\nabla [\partial \Xi / \partial \nabla g] = \partial \Xi / \partial g, \quad (9)$$

with Dirichlet boundary condition $g(\mathbf{r}) \equiv 4$ for $\|\mathbf{r}\| = R$. This condition is defined with R sufficiently large so the protein molecule is contained in the ball $\{\|\mathbf{r}\| < R', R' \ll R - 5d\}$, with $d = 2.5 \text{ \AA} \approx$ thickness of a water layer. Thus, $g(\mathbf{r})$ satisfies the Poisson-type equation:

$$\nabla^2 g = -h(\mathbf{r}), h(\mathbf{r}) = (1/\lambda) \partial \mathbf{P} / \partial g, \text{ with } g(\mathbf{r}) \equiv 4 \text{ for } \|\mathbf{r}\| = R, \quad (10)$$

that is numerically integrated [19, 20] to yield $g(\mathbf{r})$.

3. Protein-water interfacial tension determines association propensities

The solvent-accessible envelope of the protein surface [21, 22] may be covered by a minimal set W of water-confining osculating spheres D_j , $j \in W$. These spheres make first-order contact with the envelope obtained by sliding a water molecule along the surface, thus smoothening out its singularities [21]. As a minimal covering, W contains all interfacial water molecules and this

property no longer holds if any osculating sphere is excluded from the set, even though the osculating spheres may intersect. Interfacial tension arises in D_j when $\Delta G_j > 0$, where $\Delta G_j = \frac{1}{2} \int_{D_j} \{ \lambda |\nabla g|^2 - |\mathbf{P}(g(\mathbf{r}))|^2 \} d\mathbf{r}$ is the interfacial surface tension associated with spanning contact region j .

To support the claim that ΔG_{if} is a determinant of the propensity of the protein to associate, we examined free subunits in 28 protein complexes (Table 1) with defined contact topologies [5]. The total area of the P-P (protein-protein) interfaces for each complex is computed after identification of the subunit residues engaged in intermolecular contacts. Separately, ΔG_{if} for each free protein subunit is computed by numerical integration of Eq. (10) with charge and atomic radii (Eq. (5)) assigned using the program PDB2PQR [23]. We define filtered sets $W_n = \{j \in W: \Delta G_j \geq nk_B T\}$ ($n=1,2,\dots$) of contributors to the P-W interfacial tension in the free subunits ($W_n \subset W_{n'}$ for $n > n'$), with S_n , the total P-W interface associated with W_n , and A_n , the surface area of S_n . In all 28 complexes examined, the total P-P interface distributed among the subunits within the complex is 100% contained in S_2 , and it is only $60 \pm 7\%$ contained in S_3 .

These results suggest that interfacial solvent cavities spanned at a thermodynamic cost $\Delta G \geq 2k_B T$ are the promoters of protein associations. This conclusion is corroborated by the tight correlation ($R^2=0.87$) between A_2 and the total P-P interfacial area of each complex (Fig. 1). This correlation becomes weaker for S_1 with area A_1 ($R^2=0.62$) and becomes negligible ($R^2=0.19$) when we consider the total solvent-exposed surface area (SESA) [21, 22] of free protein subunits. The correlation between the areas of surface patches that significantly destabilize the protein-water interface (A_2) and those of binding sites reveals that proteins associate to reduce protein-water interfacial tension.

The interfacial tension $\gamma_{if} = \Delta G_{if}/(\text{SESA})$ of soluble nonhomologous monomeric proteins with structures reported in the Protein Data Bank (PDB) has been computed for an exhaustive dataset of 11,964 uncomplexed monomeric proteins or peptides and varies in the range $1.25 \text{ mJ/m}^2 \leq \gamma_{if} \leq$

9.90mJ/m². The list of proteins or peptides with sustainable structure is compiled in the Supporting Information of ref. [24]. The computation follows exactly the same operational premises adopted for free protein subunits from the complexes indicated in Table 1: The protein-water interface is decomposed into a minimal covering of osculating spheres making first-order contact with the solvent-accessible envelope, and the free energy cost of spanning each interfacial sphere, ΔG_j , is computed as described above with the field g determined for each protein structure by numerical integration of Eq. 10. Strikingly, the maximum γ_{if} -value corresponds to the cellular metastable fold of a prion protein (PDB.1qm0), capable of promoting phase separation through fibrillogenic aggregation [25].

Hot spots in P-P associations were identified by scanning the interface through site-specific substitution of amino acids for alanine (effectively a side-chain truncation) [6]. An extensively scanned interface corresponds to the human growth hormone (hGH)-receptor complex (Fig. 2). To validate our molecular marker, the hot spots obtained by alanine scanning were contrasted with an *in-silico* side-chain truncation procedure (side-chain groups beyond β -carbon are removed) that determines a reduction in interfacial tension, $\Delta\Delta G_{if} = \Delta G_{if}(m) - \Delta G_{if}(0)$, caused by a site-directed mutation (0=wild type \rightarrow m=mutation). The side-chain truncation at the β -carbon is equivalent to the alanine substitution in the experimental dissection of the interfacial hot spots. A strong correlation exists between the terms $-\Delta\Delta G_{if}$ and the association free energy difference $\Delta\Delta G_a$ experimentally obtained from substitution of interfacial residues (Fig. 3). Thus, inferred tension patches coincide with hot spots at complex interfaces identified by mutational scanning.

4. Conclusions

The aqueous biological interface is physically heterogeneous and geometrically confined at multiple scales. For these reasons, no generic thermodynamic concept like interfacial tension, broadly used in the context of homogeneous phase separation, can be directly determined without

a surface integration procedure. This work provides the theoretical framework to enable such integration. The biological interfacial tension is unique in that biological solutes may form obligatory, ephemeral or adventitious complexes but never precipitate under physiological conditions. The only distinct phase separation encountered in biology appears to be the amyloidogenic aggregation of prions [9, 25], which as noted in this work, are endowed with a soluble structure generating the highest protein-water interfacial tension.

Since protein-water interfaces are highly heterogeneous both physically and geometrically, broad classifications of proteins into hydrophilic, amphiphilic and hydrophobic classes are not very helpful at understanding biomolecular interactivity and the fact that complexation (and not precipitation) is always the evolutionary solution to the need for functional regulation and cooperativity. In broad terms we could say that, for identical local curvature, a hydrophilic patch is more likely to reduce interfacial tension than a hydrophobic patch since the latter curtails the hydrogen bonding opportunities of interfacial water ($g < 4$). However, interfacial tension is also defined by local curvature: a hydrophilic patch introducing favorable polarization may be partially hindered from hydration due to local geometric constraints and thus, the local interfacial g -value may be lower than the bulk value $g=4$, contributing to the interfacial tension.

The protein-water interfacial tension may be modulated by the cellular machinery to alter complexation propensities, and hence the degree of functional cooperativity and regulation, in a purposely choreographed manner. Thus, glycoslation and phosphorylation are two ubiquitous post-translational modifications of proteins that increase hydrophilicity by transesterification of solvent-accessible specific side chains (serine, threonine and tyrosine). These processes generally decrease the protein-water interfacial tension by increasing the number of favorable interactions with interfacial water.

The results presented in Figs. 1-3 uphold the variational treatment of biological water and highlight the relevance of protein-water interfacial tension as determinant of protein associations. The polarization and elastic terms are defined respectively by a sub-microscopic (τ_b) and a

macroscopic (λ) parameter. While the latter is fixed, the former is adjustable, since dielectric loss spreads over the microwave range, yet the adopted value $\tau_b=100\text{ps}$ (wavelength $\approx 0.03\text{m}$) yields the optimum prediction of binding sites (Figs. 1, 3).

The variational principle derived incorporates an elastic term to penalize local losses in water hydrogen-bond coordination and was shown to govern nanoscale configurations of water at biological interfaces. In consonance with a nanoscale description, the treatment allows for compensations to the elastic penalization as water dipoles interact with the electrostatic field in a more or less restricted manner depending on their individual coordination environments. The extremal of the functional that underlies the variational principle determines the expected hydrogen-bond coordination $g(\mathbf{r})$ of water at a given position \mathbf{r} in space. This scalar field g is easily determined numerically once it is shown that it obeys a Poisson-type equation with Dirichlet boundary conditions.

These findings may impact the field of biomaterial self-assembling, since molecular fabrication is determined by the structural compatibility of subunits that confers noncovalent interactions [26]. These organizing interactions are promoted by the propensity to reduce protein-water interfacial tension. While the charge distribution will be altered upon protein association and the interfacial tension will change accordingly, such interactions can be in principle engineered by introducing patches of high protein-water interfacial tension in the basic subunits.

Acknowledgments

This work was partially supported by funds from the Institute of Biophysical Dynamics and the Computer Science Department at The University of Chicago and by the National Research Council of Argentina (CONICET). The author is grateful to Prof. Ridgway Scott for valuable discussions.

Table 1



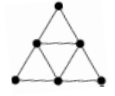



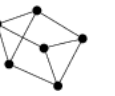










 2af7 (63)	 1fr3 (61)	 2siv (59)	 1ub4 (53)	 2a1b (51)	 2c5r (40)	 4otc (57)
 1qoh (54)	 1dvz (57) 1jtk (55)	 1hho (64)	 1nys (39)	 1uo5 (54) 1vwe (53)	 1fvu (50)	 1zij (52) 1ufy (51)
 1wud (42)	 1u4j (48) 1hpo (56) 1htg (50) 1lve (47) 2oqq (60) 1v2z (51) 1btn (62) 2ien (59) 1ihb (57) 1p6z (72)			 3orc 1b8x 2gfh 1goc 2b65 1h5m 1may 1uga 1quz		

Table 1. Representative topologies of inter-subunit contacts for 28 protein complexes reported in PDB. The dataset is used to unravel the role of P-W interfacial tension patches as promoters of protein associations. In the topological representation of a complex, a ball represents a protein subunit and a stick between two balls represents a protein-protein (P-P) interface. Numbers in brackets denote % decrease in overall interfacial tension upon complexation starting with free subunits.

Figure Captions

Figure 1. Protein-water interfacial tension promotes biomolecular associations. Total area of surfaces generating protein-water (P-W) interfacial tension in free subunits (uncomplexed state) plotted against the total protein-protein (P-P) interfacial area for 28 protein complexes (Table 1). Datapoints with ordinates given by areas A_1 , A_2 and solvent-exposed surface area (SESA) are represented with diamonds, triangles and squares, respectively. The linear fit with correlation coefficient $R^2=0.871$ for A_2 -(P-P interface) points was obtained by linear regression. **Inset.** Correlation coefficient R^2 as a function of bulk wavelength parameter τ_{bc} . The correlations were examined at bulk wavelengths over various orders of magnitude spanning the microwave range (wavelengths 10^{-3} m to 0.3m). The data is best correlated at $\tau=\tau_b=100$ ps, with wavelength ≈ 0.03 m, the adopted parameter value.

Figure 2. The P-P interface between the human growth hormone (hGH, ribbon) and its receptor (backbone line) in the 1:1 complex [6].

Figure 3. Comparison with experimental alanine scanning of the P-P interface of the hGH receptor validates the interfacial tension computation. Correlation between association free energy differences $\Delta\Delta G_a$ between mutant (m) and wild type (0) for the alanine substitution of each residue from the hGH receptor at the P-P interface and the interfacial free energy difference between wild-type and mutant for the free protein subunit (uncomplexed hGH receptor). The association free energy is computed as $\Delta G_a = -RT\ln K_a = RT\ln(K_d)$, where K_a , K_d are respectively the association and dissociation equilibrium constants. **Inset.** Correlation coefficient R^2 as function of bulk wavelength parameter τ_{bc} . The dependence was examined over several orders of

magnitude spanning the microwave range (wavelengths 10^{-3}m to 0.3m). Optimal correlation is achieved at $\tau=\tau_b=100\text{ps}$, wavelength $\approx 0.03\text{m}$, the adopted parameter value.

References

- [1] Ashbaugh H S and Pratt L R 2006 *Rev. Mod. Phys.* **78** 159
- [2] Despa F 2005 *Ann. N. Y. Acad. Sci.* **1066** 1
- [3] Gerstein M and Chothia C 1996 *Proc. Natl. Acad. Sci. U.S.A.* **93** 10167
- [4] Giovambattista N, Lopez C F, Rossky P and Debenedetti P G 2008 *Proc. Natl. Acad. Sci. U.S.A.* **105** 2274
- [5] Levy E D, Pereira-Leal J B, Chothia C and Teichmann S A 2006 *PLoS Comput. Biol.* **2** e155
- [6] Clackson T, Ultsch M H, Wells J A, and de Vos A M 1998 *J. Mol. Biol.* **277** 1111
- [7] Frauenfelder H *et al.* 2009 *Proc. Natl. Acad. Sci. U.S.A.* **106** 5129
- [8] Fenimore P W, Frauenfelder H, McMahon B H and Young R D 2004 *Proc. Natl. Acad. Sci. U.S.A.* **101** 14408
- [9] Fernández A 2010 *Transformative concepts for drug design: Target wrapping*. Springer, Heidelberg.
- [10] Rowlinson J S and Widom B 1982 *Molecular Theory of Capillarity*, Oxford University Press, New York.
- [11] Stillinger F H 1973 *J. Solution Chem.* **2** 141
- [12] Capra J A, Laskowski R A, Thornton J M, Singh M and Funkhouser T A 2009 *PLoS Comput. Biol.* **5** e1000585
- [13] Schulz E, Frechero M, Appignanesi G and Fernández A 2010 *PLoS One* **5** e12844
- [14] Kumar P, Buldyrev S V and Stanley H E 2009 *Proc. Natl. Acad. Sci. USA* **106** 22130

- [15] Hasted J B 1972 in *Water: A comprehensive treatise*, vol. 1, F. Franks, ed., Plenum Press, New York, pp. 255-309.
- [16] Buchner R, Barthel J and Stauber J 1999 *Chem. Phys. Lett.* **306** 57
- [17] Debye P 1929 *Polar Molecules*, Dover Publications, New York
- [18] Scott R, Boland M, Rogale K and Fernández A 2004 *J. Phys. A* **37** 9791
- [19] Johnson C 1987 *Numerical solution of partial differential equations by the finite element method*. Cambridge University Press, Cambridge, UK
- [20] Persson P O and Strang G 2004 *SIAM Rev.* **46** 329
- [21] Street A G and Mayo S L 1998 *Fold. Des.* **3** 253
- [22] Zhang N, Zeng C and Wingreen N S 2004 *Proteins Strct. Funct. Bioinf.* **57** 565
- [23] Dolinsky T J, Nielsen J E, McCammon J A and Baker N A 2004 *Nuc. Ac. Res.* **32** W665
- [24] Fernández A and Berry R S 2010 *J. Proteome Res. (ACS)* **9**, 2643
- [25] Zahn R *et al.* 2000 *Proc. Natl. Acad. Sci. USA* **97** 145
- [26] Zhang S 2003 *Nat. Biotechnol.* **21** 1171

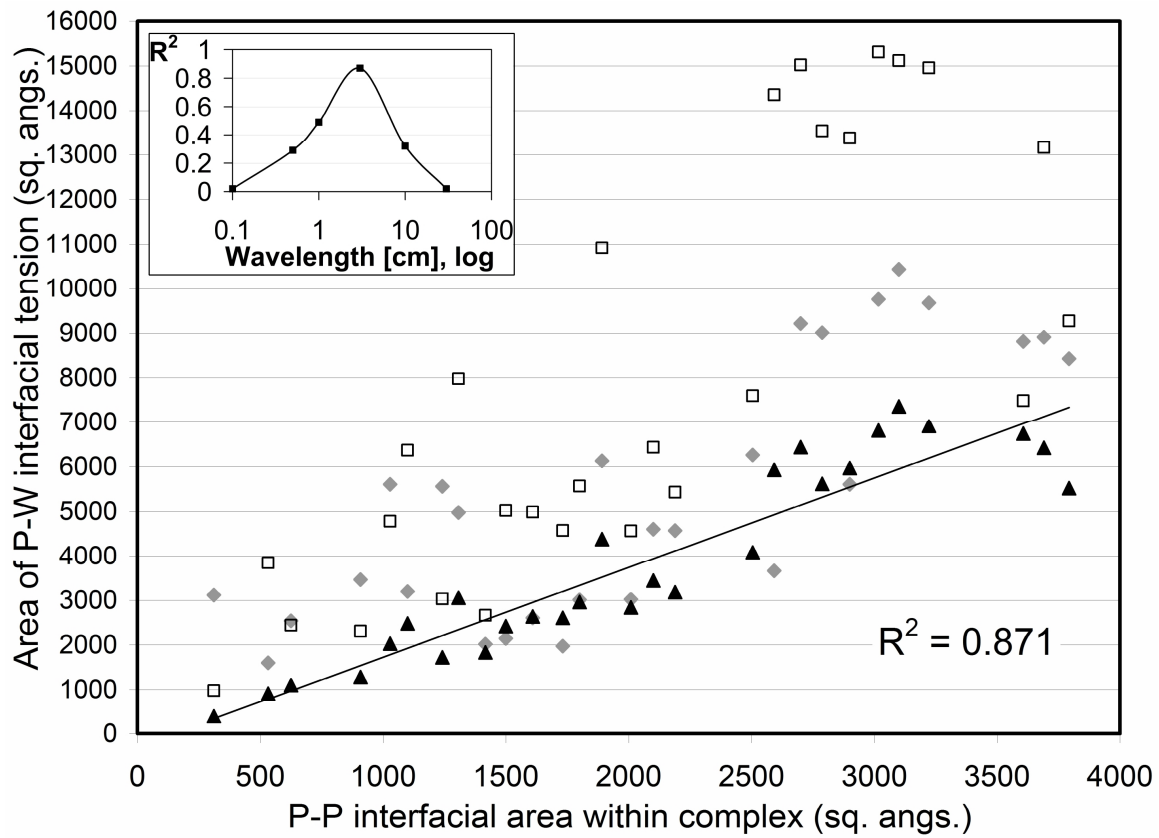


Figure 2

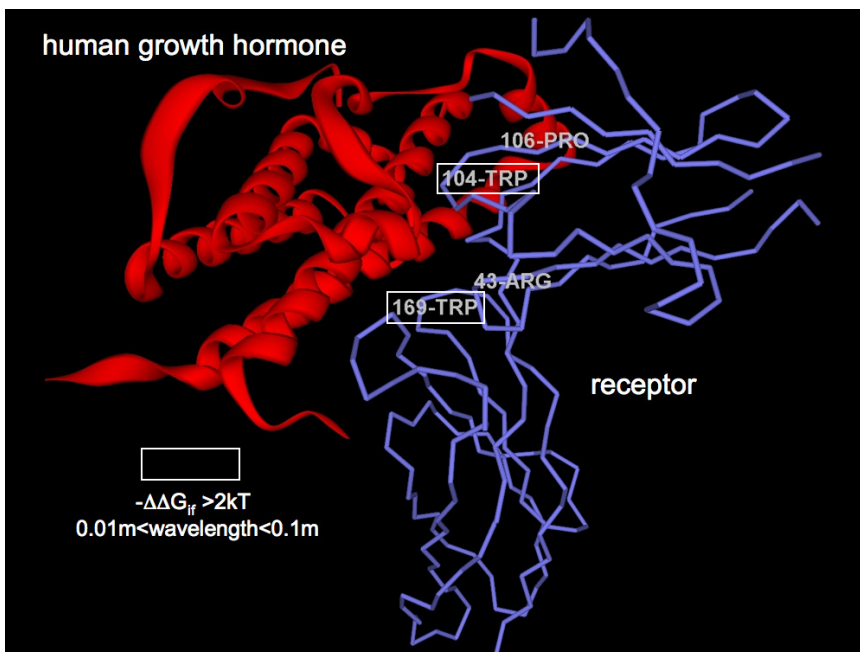


Figure 3

